

Tomographic imaging of a seismic cluster in northern Taiwan and its implications for crustal fluid migration

Win-Bin Cheng (wbin@just.edu.tw)

Department of Environment and Property Management, Jinwen University of Science
and Technology

Abstract

After the occurrence of the 1999 magnitude 7.3 Chi-Chi earthquake, a cluster of NE-SW trending earthquakes, almost along the surface trace of the Lishan fault, has been detected in the northern portion of the Central Range in northern Taiwan. From the spatiotemporal distribution of hypocenters based on cluster analysis, the Lishan fault cluster (LFC) can quantify the evolution of seismicity as aftershocks of the 1999 Chi-Chi earthquake. The results of seismic tomographic inversion indicate that the LFC extends down to about 10 km depth and seems to be distributed in high V_p areas rather than in low V_p areas. This temporal expansion is attributed to fluid diffusion. Seismic activity in the upper crust tends to be high above broad zone with low V_p in the lower crust. Our tomographic images demonstrate a series of relatively high V_p/V_s anomalies dipping to the east which seems to form a fluid upwelling conduit beneath the Central Range. We thus suggest that the Lishan Fault might play a role of an active fluid conduit, fluid or fluid fluxed a partial melt of the Philippines Sea plate would be released along the east-dipping conduit and rise gravitationally to the upper crust.

Keywords: Seismic tomography, Lishan Fault, fluid migration

1. Introduction

Earthquakes generate stress perturbations that can promote subsequent

events and trigger aftershocks. Earthquakes generally involve a variety of coseismic and post seismic responses, in which stress changes and triggered aftershocks can provide insight into Earth's internal fluid migration or aseismic slip (e.g., Lohman and McGuire, 2007; Chen et al., 2012). Increasing in fluid pressure will reduce the effective normal stress, effectively weakening the fault and shear strength to a level below the prevailing shear stress (Sibson, 1991). Therefore, earthquakes may be correlated to pore pressure diffusion and stress transfer (Byerlee, 1978; Byerlee, 1990; Rice, 1992; Hainzl, 2004; Miller et al., 2004; Cappa et al., 2009; Okada et al., 2015) that may reduce crustal strength and promote a great number of earthquakes with a large range of magnitudes (Roeloffs, 2000; Sibson, 2013).

On 21 September 1999, a $M_w = 7.6$ magnitude earthquake occurred in the western foothills of central Taiwan, near the small town of Chi-Chi ($120.89^\circ\text{E}/23.82^\circ\text{N}$, depth of 8–10 km) (Ma et al., 1999) and produced a complex surface rupture extending over 80 km. The focal mechanism and fault ruptures indicate thrusting on a fault striking N-S roughly parallel to the mountain belt (Kao and Chen, 2000). Coseismic surface deformation and significant change in shallow seismic activity in the crust around the source area are also reported (Ma et al., 1999; Wang, 2000; Dominguez et al., 2003; Yu et al., 2003; Rousset et al., 2012).

Figure 1 shows the change of seismicity before (1991-1998) and after (2005-2012) the Chi-Chi earthquake. Most of the earthquake clusters were activated after the Chi-Chi earthquake, especially the Lishan fault cluster (Fig. 2). Wang (2000) shows that the static stress field changed because of the large slip caused by the Chi-Chi earthquake. However, some of the earthquakes in the northern Taiwan has focal mechanisms that do not correspond to the stress change by the Chi-Chi earthquake. We know that pore-fluid pressure is another factor that controls the occurrence of earthquakes (Sammonds et al., 1992; Beeler et al., 2000; Miller et al., 2004;

Okada et al. 2011). In particular, hypocenter migration can be attributed to the fluid diffusion process (Shapiro et al., 1997; Yukutake et al. 2011; Chen et al. 2012; Hardebeck 2012; Okada et al. 2015). In this study, we will consider some possible evidence of the influence of crustal fluid/water on the occurrence of the triggered seismicity after the Chi-Chi earthquake. We use tomographic models of V_p and V_p/V_s to examine possible causes of the seismicity clusters and their relationship to the movement of fluids through part of the collision/subduction system.

3. Results and Discussion

In crustal structure, V_p and V_p/V_s velocities are dependent on several factors, such as composition, pressure, temperature, crack density, pore pressure and fracture distribution. In addition, the V_p/V_s has been used as an indicator of fluids within many tectonic settings, such as collision zones (Huang et al., 2014), subduction zones (Zhao et al., 1992; Husen and Kissling, 2001), shear zones (Zhang and Lin, 2014) and volcanoes (Koulakov et al., 2009). Several studies have indicated that fluids may also play a role in the arc magmatism and periodic swarms (Nakajima et al., 2009; Hainzl et al., 2012).

We plot a series of vertical cross sections of the V_p , V_p/V_s profiles almost perpendicular to the trend of the Lishan fault (Fig. 6 and Fig. 7). Earthquake events with magnitude ≥ 2.0 recorded from 1991 to 2015 were relocated with the CWB 3-D velocity model within a 10-km distance from each cross section are also plotted. The preliminary results are: 1) high V_p and V_p/V_s heterogeneities are observed beneath the Lishan fault; 2) Lishan fault cluster (LFC) has a much less vertical extent that extends down to about 10 km depth above low V_p areas (Fig. 6); 3) a relatively high V_p/V_s zone is observed beneath the Lishan fault. A series of relatively high V_p/V_s anomalies increase its depth from west to east beneath the Lishan fault and northern portion of the Central Range (see clearly in Fig. 7c and 7d); 4)

earthquake hypocenters occurred in the crust east to 121.5°E is generally fall within relatively high V_p and high V_p/V_s zones.

4.1 Relationship Between Fault Zone Structure and Seismicity

Large velocity variations are imaged in the study area. In the upper crust, there are many distinct seismic low-velocity areas. These low-velocity areas are distributed in and around the Foothill zone and northern portion of the Lishan Fault (Fig. 6). It is worth noting that the Lishan Fault could be characterized by clear lateral V_p and V_p/V_s variations in the top 10 km of the crust (Figs. 6 and 7). Combine field observation of geological structure and regional paleostress analyses, Lee et al. (1997) suggested that the Lishan Fault zone underwent polyphase evolution with reactivations under different tectonic regimes. It shows contrasting evidences of being a major normal fault, a major reverse fault, and also a sinistral strike-slip fault during the Cenozoic deformation. Stratigraphic studies revealed a significant contrast between the formations on the western and eastern sides of the fault (Teng et al., 1991). This is consistent with the prominent features along Y90 profile where the V_p and V_p/V_s change from 4.8 to 5.6 km/s and 1.67 to 1.74, respectively at about depth of 7 km beneath the Lishan Fault.

In the upper crust, the LFC extends down to about 10 km depth and seems to be distributed in relative low V_p and high V_p/V_s areas (Y70 and Y80 in Figs. 6 and 7). V_p/V_s is useful information for understanding the fluid migration (e.g., Husen et al. 2000; Zhao et al. 2002; Zheng and Lay, 2006). High V_p/V_s zones have often been interpreted as regions of high pore fluid pressure, where low V_p/V_s areas can be interpreted as high aspect-ratio pores with water or gas (Spencer and Nur, 1976; Musacchio et al., 1997; Kodaira et al., 2004; Audet et al., 2009; Peacock et al., 2011). High V_p/V_s feature is significant beneath the Lishan fault. The Lishan Fault is a major structural boundary and highlights the importance of preexisting features in the

development of the Taiwan orogen (Ho, 1982; Teng et al., 1992; Gourley et al., 2007; Van Avendonk et al., 2016). Taking into account these studies, we consider that the low- V and average to slightly high Poisson ratio under Kii Peninsula at crustal depths are related to the presence of fluids.

High V_p/V_s areas are distributed also in and around the earthquakes beneath the offshore region (Fig. 7). However, most of the earthquakes occurred below the onshore region are located around these low- V_p/V_s areas. From upper crust to lower crust, the lateral V_p/V_s variation is evidence that located just beneath the east coast. A clear-cut edge of seismicity is consistent with Ustaszewski et al. (2012) that confining the northward dipping Philippine Sea plate and abuts the plate interface is significant in our V_p/V_s images (Fig. 7).

The Lishan Fault zone underwent polyphase evolution with reactivations under different tectonic regimes, consistent with the Cenozoic history of Taiwan. The curved zone delineated by the lateral V_p variations shows a pattern dipping to the east in Y70 and Y80 profiles (Fig. 6), whereas the curved zone show a high-angle westward dipping trend in Y90 to Y110 profiles (Figs. 6). Lee et al. (1997) suggested that a transformation to back-thrusting of the Lishan Fault is considered a combination of the Quaternary rapid uplifting of the Hsüehshan Range and the continuation of the horizontal compression in the Taiwan mountain belt. The early stage of the Lishan Fault in west-vergent reverse and strike-slip fault (Fig. 8b) probably occurred with a steep inclination of the fault surface structure which has a mechanical tendency to turn to east-vergent thrusting near the surface during uplifting of the Hsüehshan Range. Late N-S extension occurred in the northern segment of the Lishan Fault (near the Ilan Plain), suggesting that its most recent mechanisms are influenced by the N-S back-arc opening of the Okinawa Trough northeast off Taiwan during the last 2 Ma (Letouzey and Kimura, 1986; Liu, 1995).

Based on long-period magnetotelluric measurements, Bertrand et al. (2012) reported that Lishan fault conductor domain is characterized by an area of anomalously low resistivity. In addition, the northern portion of the Lishan fault should be an extensional regime which is probably produced by a clockwise rotation of the “northern Central Range” block associated with the northwestward collision of the Luzon Arc against the Eurasian continental margin (Yu et al., 1997; Ku et al., 2009).

In the lower crust (Fig. 6), we found seismic low-velocity areas that appear to be elongated along NE–SW, the strike of the Taiwan mountain belt. These seismic low-velocity areas are located not only beneath the Central range but also beneath the Foothill zone. Seismic activity in the upper crust tends to be high above these low-velocity areas in the lower crust. Based on interpretations of geological and geophysical data, the Lishan fault is a geologically complex, steeply west dipping structure whose geophysical signature indicates that it can be traced into the middle and perhaps even the lower crust (Clark et al., 1993; Lee et al., 1997; Bos et al., 2003; Wu et al., 2004; Bertrand et al., 2012).

It has been pointed out that fluid flow is closely associated with the occurrence of earthquake cluster in several regions. It has been suggested that the migration of the hypocenter area is related to fluid in several studies, e.g., the 1989 Dobi earthquake sequence of central Afar (Noir et al., 1997), in the West Bohemia/Vogtland region (Špičák and Horálek, 2001; Fischer and Horálek, 2003), in the Tjörnes fracture zone in North Iceland (Hensch et al., 2008), and the 2011 M9.0 Tohoku-Oki earthquake in Japan (Yoshida et al. 2012; Yukutake et al. 2011; Okada et al. 2015). In general, most of the earthquake clusters were activated in the upper crust. We found distinctly seismic low V_p and high V_p/V_s areas below the seismically active area (the earthquake cluster) in Figures 6 and 7. This seismic low-velocity area could

correspond to an area with overpressurized fluids, and migration of overpressurized fluids from there would promote the occurrence of earthquakes. Magnetic anomalies and the focal mechanism of 14 events with depth less than 10 km and magnitudes greater than 4.5 are plotted on the 7-km depth Vp and Vp/Vs slices in Figure 8. Most of the shallow earthquakes, including the normal fault earthquakes in northern Taiwan after the occurrence of the 1999 Chi-Chi earthquake, are generally within relatively high Vp and high Vp/Vs zones. It is interesting that those normal fault earthquakes and earthquake clusters occurred in an area where the high magnetic belt is blurred (Fig. 8c). The relationship between the sharp truncation in the observed magnetic field with the earthquake clusters, normal faulting, fluid migration, and the collision of the Philippine Sea plate and the Eurasian continent require further study. The mainshock was located in or near the junction between low-velocity and high-velocity zones (Figs. 8 and 9) where the mechanical strength of materials is much weaker than that in normal sections of the seismogenic layer due to the penetration of fluids from the lower crust. Thus the margin of a crustal block is an ideal location to generate large earthquakes that produce faults that reach to the Earth's surface or blind faults within the brittle upper crust

2 Localized Upwelling beneath the Lishan fault

Lishan Fault is a major structural boundary and highlights the importance of preexisting features in the development of the orogen (Gourley et al., 2007; Van Avendonk et al., 2016) and an inverted passive margin growth fault that shows oblique thrust movement (Angelier et al., 1990; Clark et al., 1993; Lee et al., 1997). Further, observation and analysis of foliated rocks with extensive veining suggest that the Lishan Fault hosts an active fluid flow system (Upton et al., 2011). A low resistivity was observed beneath the

Lishan fault which extends beyond a depth of 10 km and represents a distributed zone of saline fluids in the middle to the lower crust (Bertrand et al. 2012). A number of previous studies have suggested that seismicity commonly occurring at the perimeters of conductors interpreted as zones of fluids (e.g., Ogawa et al., 2001; Bertrand et al., 2009; Wannamaker et al., 2009). Deep subduction-generated fluids could rise from the mantle and invade upper crustal seismogenic zones on high-angle thrusts (e.g., Wannamaker et al., 2009). Our tomographic images demonstrate a series of relatively high V_p/V_s anomalies increase its depth to the east of the profiles which seems to form a fluid upwelling conduit beneath the Lishan fault and northern portion of the Central Range (Fig. 7c and 7d). If the Lishan Fault plays a role of an active fluid conduit, fluid or fluid fluxed a partial melt of the Philippine Sea plate would be released along the east-dipping conduit and would rise gravitationally to the area of earthquake cluster (Fig. 9). Further, if a low resistivity feature of the Lishan fault is caused by a zone of interconnected aqueous fluids, then this is significant with the depth extent of deformation in central Taiwan (Bertrand et al. 2012).

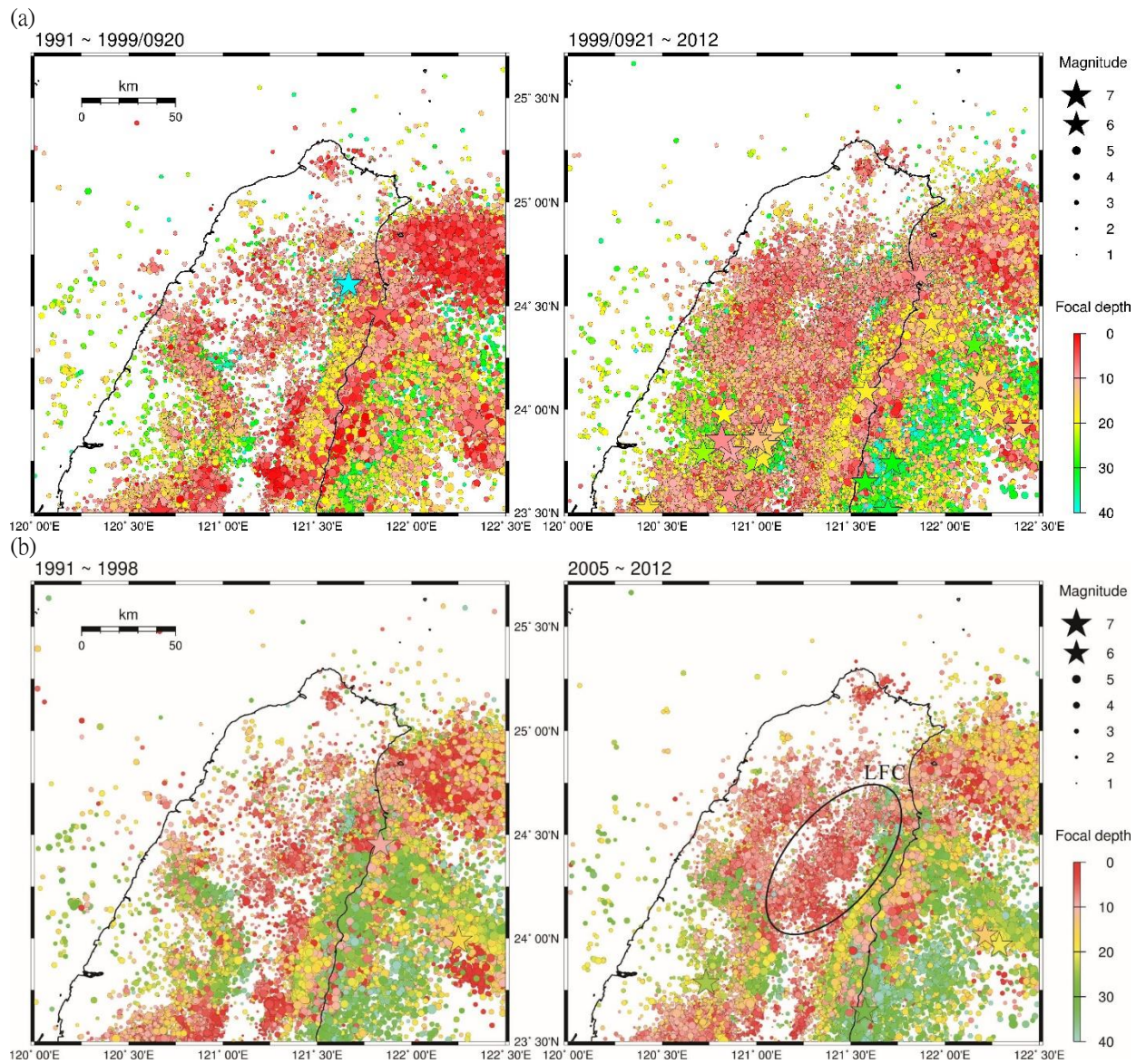


Figure 1. Map showing seismicity of the northern Taiwan based on earthquake data recorded by the Central Weather Bureau Seismic Network before (left) and after the 1999 Ch-Chi earthquake. Earthquake epicenters are color-coded by depth intervals shown on right. LFC: Lishan fault cluster.

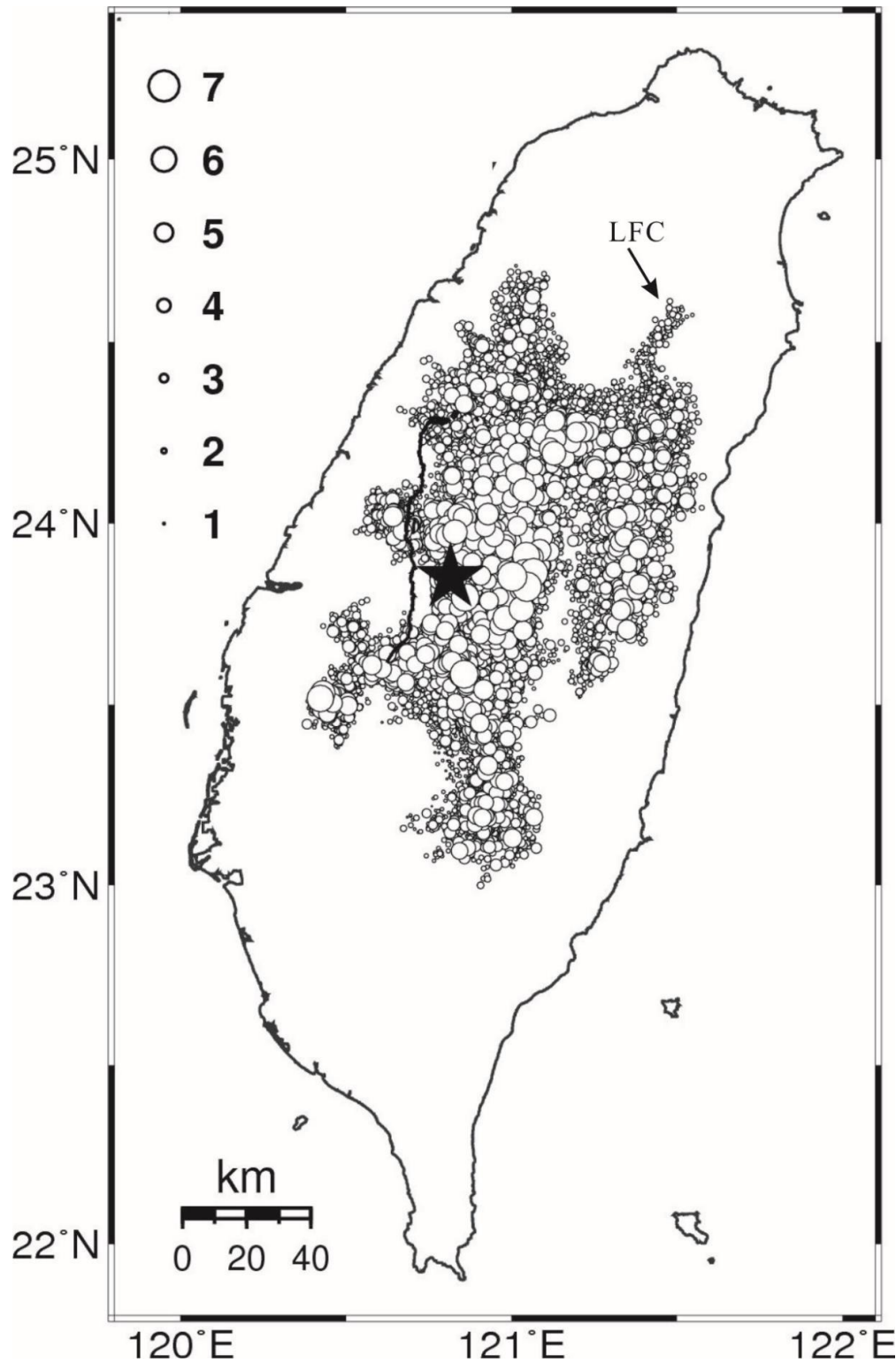


Figure 2. (a) Map of earthquake epicenters, $M_L \geq 2$, from the relocated catalog of the Central Weather Bureau and (b) Time history of Lishan Fault cluster with magnitude, LFC composed of earthquake swarms rather than mainshock-aftershock sequences. It illustrate visually various changes of seismic intensity, most clearly related to aftershock sequences of the Chi-Chi earthquakes. Circle size is proportional to magnitude. LFC: Lishan Fault cluster.

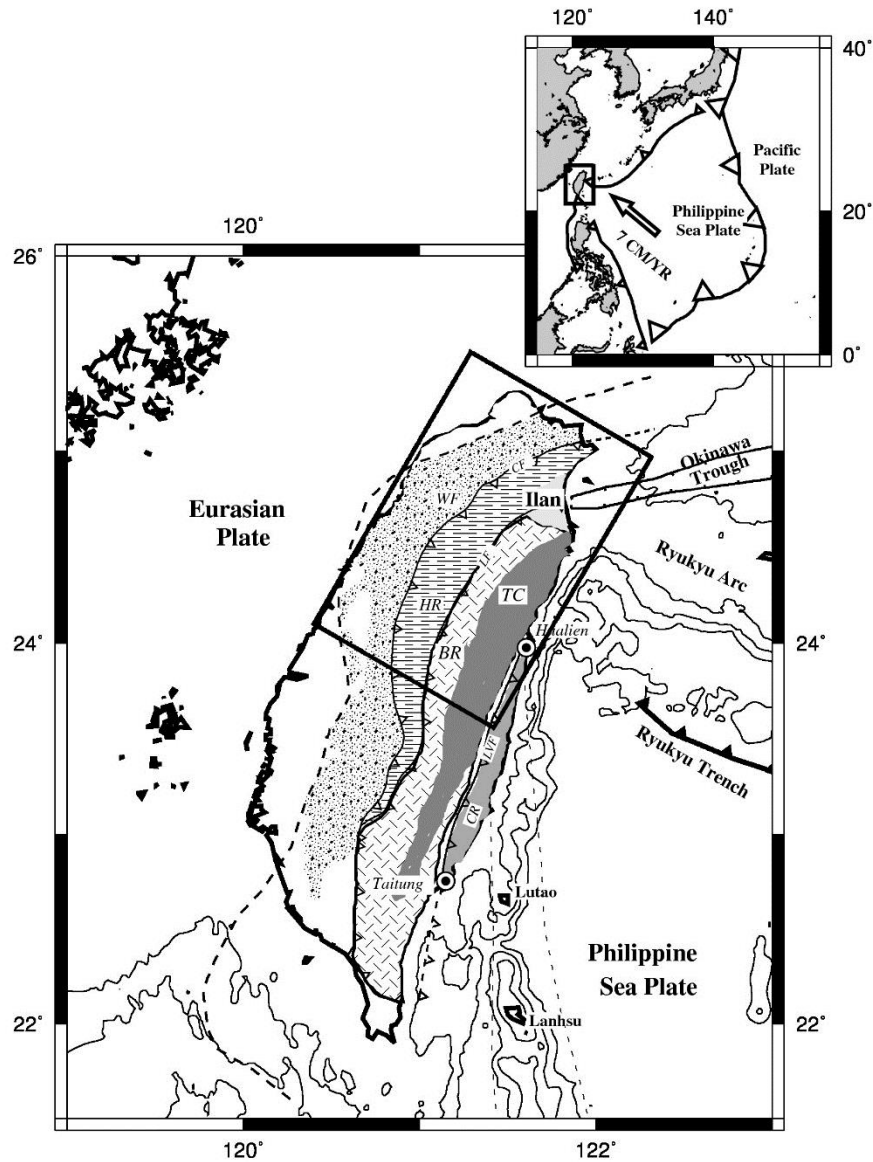


Figure 3.

Figure 3. Tectonic sketch map and bathymetry of the Taiwan region and location of the sections (geodynamic setting in the upper-right). Solid square indicates the study area. Major thrust faults with open triangles on the upper side. Arrows indicate velocities of GPS stations relative to Penghu (Yu et al. 1997). BR- Backbone Range; HR-Hsueshan Range; CR-Coastal Range; WF-Western foothills; TC-Tananao Complex; LF – Lishan fault; CF – Chuchih fault; LVF – Longitudinal Valley fault.

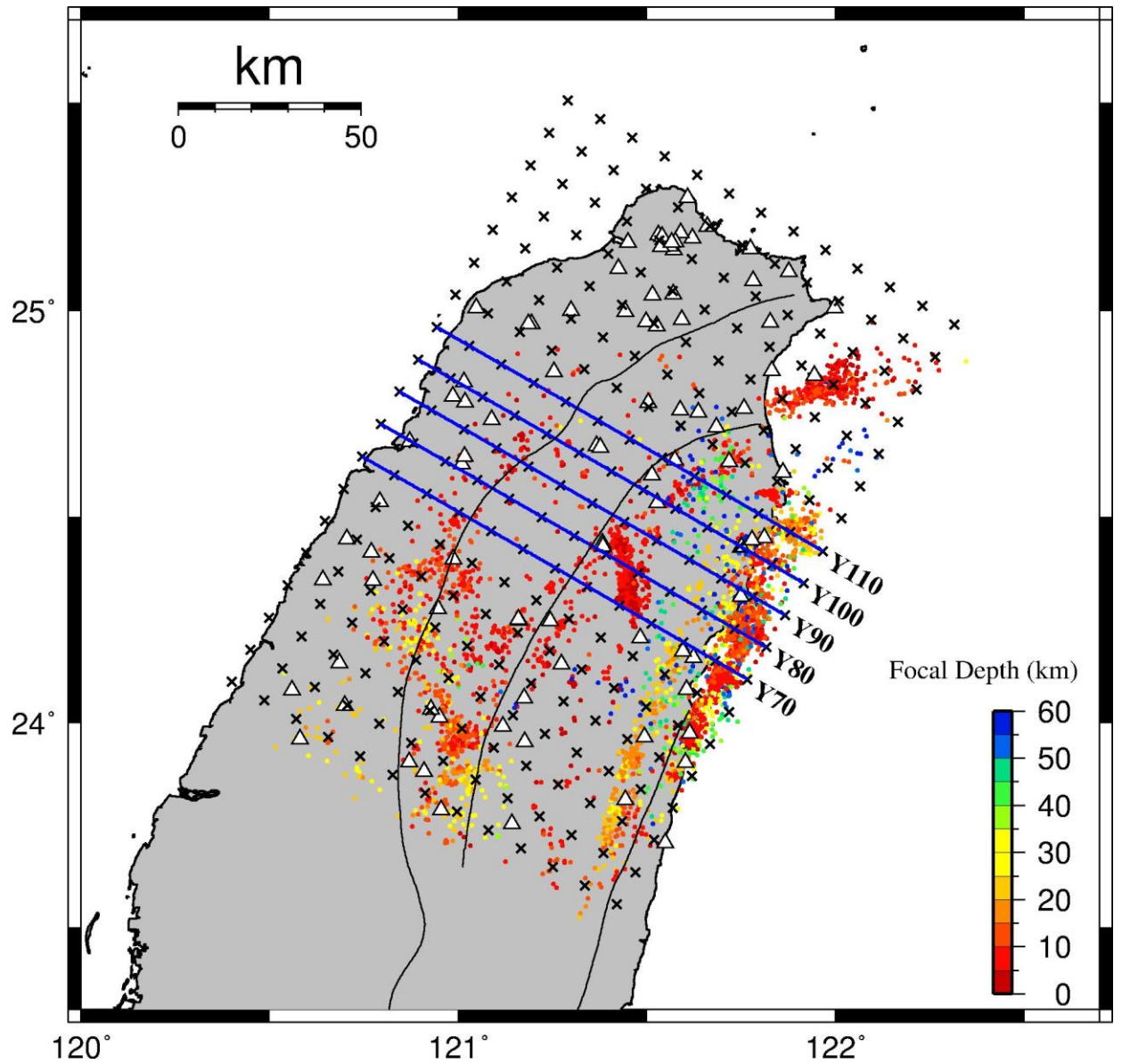


Figure 4. (a) Grid nodes (crosses) and earthquakes (solid circles) used in the three-dimensional inversion. Inverted open triangles denote stations of the Central Weather Bureau Seismographic Network. Location of velocity profiles Y70 to Y110 are shown in Figures 6 and 7.

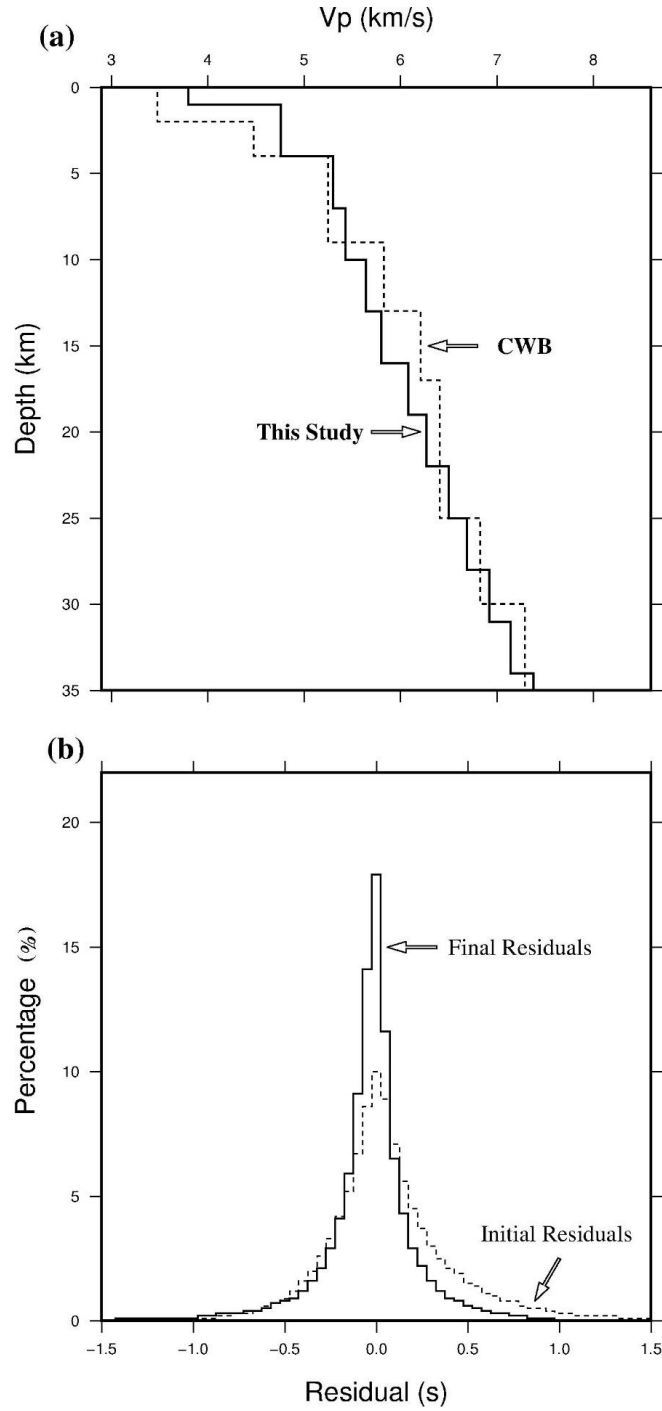


Figure 5. Results of checkerboard resolution tests for Vp/Vs model. The models recovered using seismic traveltimes are shown from 4-km to 31-km in depth. Grey colors denote slow and fast velocities, respectively. The depth of each layer is shown at the upper-left part of the map. The grid spacing is 10 km in the horizontal direction. The perturbation scale is shown on the right.

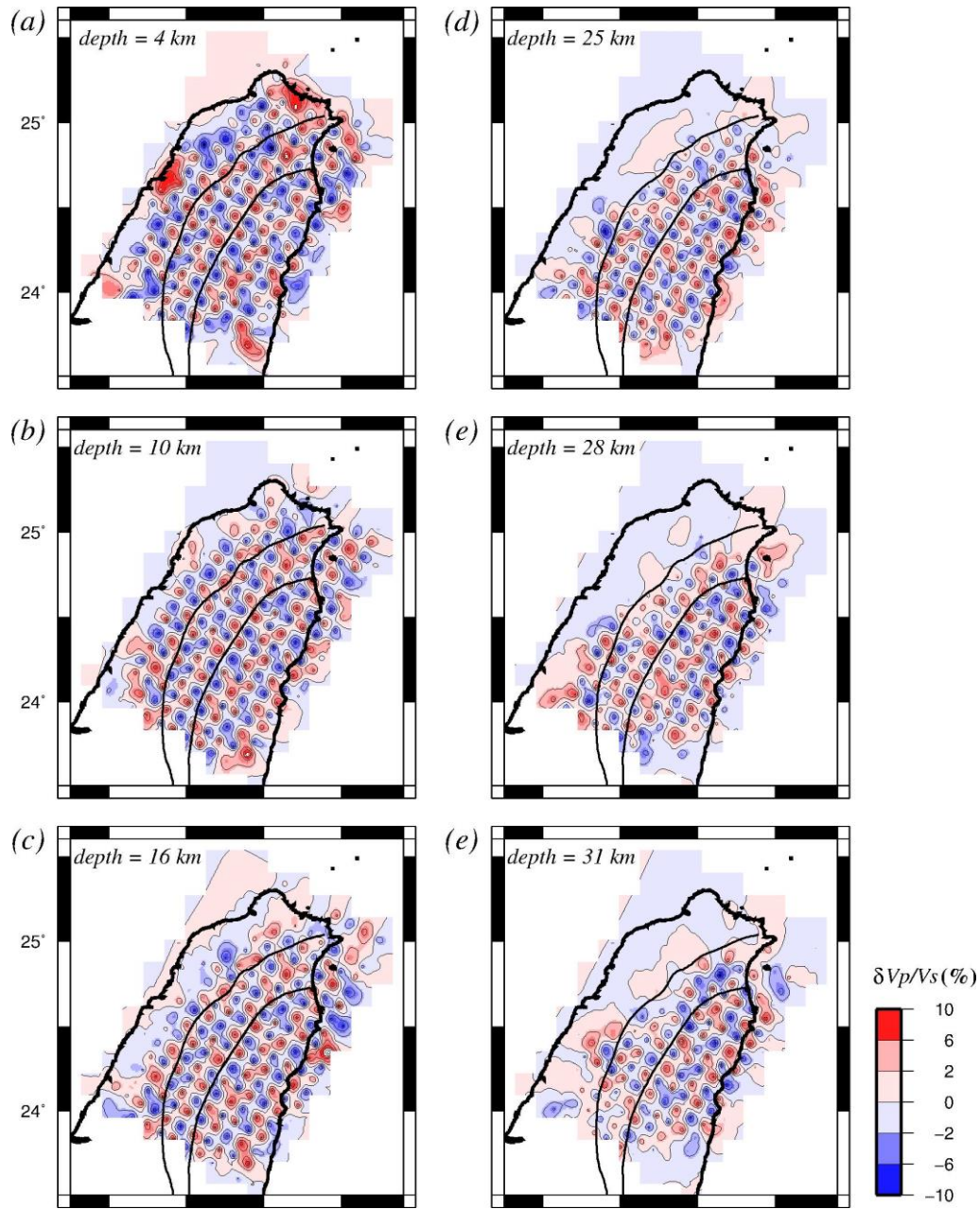


Figure 6. Vertical cross-sections of P-wave velocity (left) and checkerboard resolution test (right) along profiles from (a) north (Y110) to (e) south (Y70) sections as shown in Fig. 4. The starting checkerboard model with a $\pm 10\%$ variation in P-wave velocity. Blue and red denote relatively fast and slow velocities, respectively.

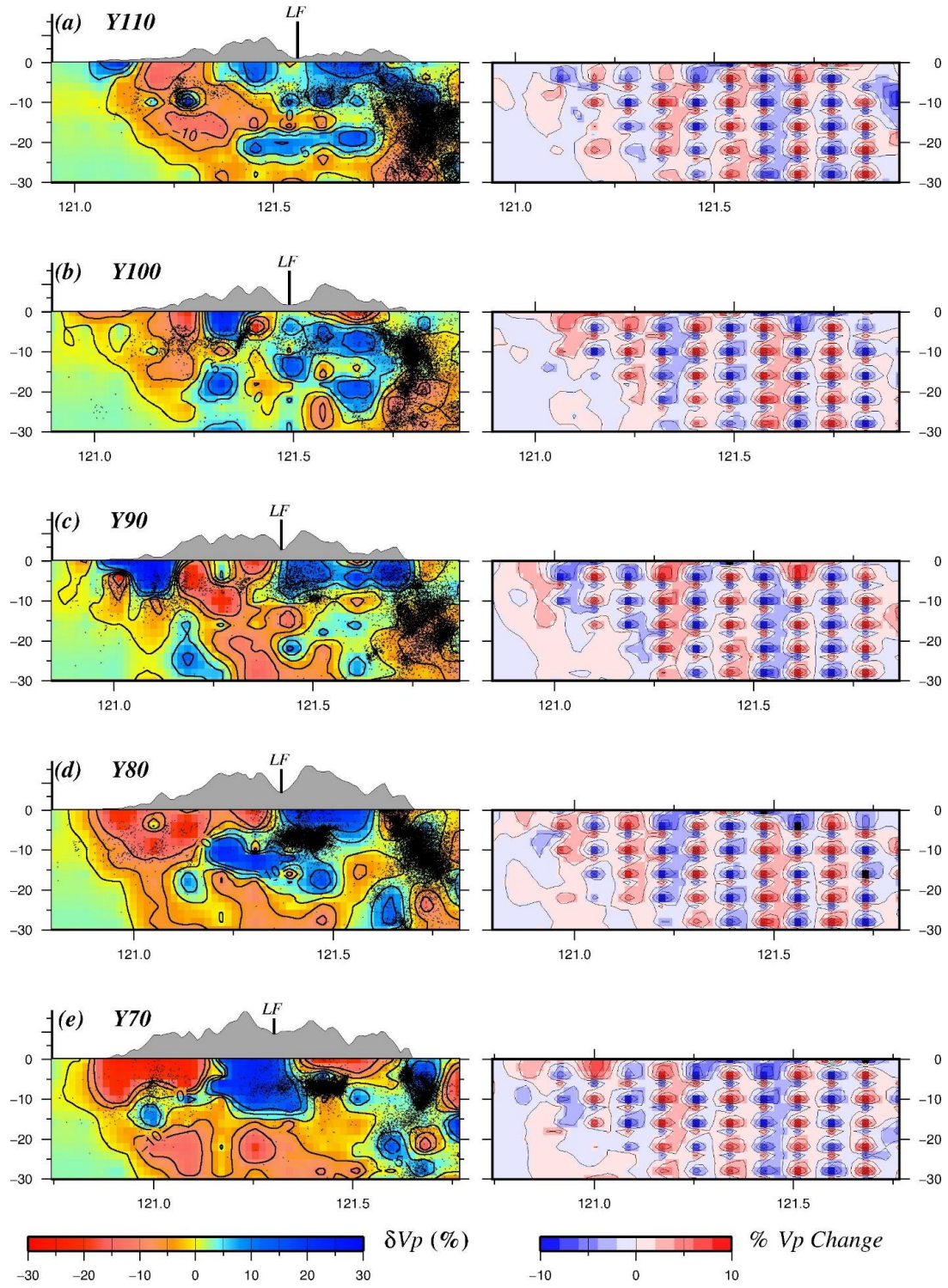


Figure 7. Vertical cross-sections of Vp/Vs (left) and checkerboard resolution test (right) along profiles from (a) north (Y110) to (e) south (Y70) sections as shown in Fig. 4. The starting checkerboard model with a $\pm 10\%$ variation in Vp/Vs. Blue and red denote low and high values, respectively. Topography of each section is shown on top. Open circles indicate relocated hypocenters. LF – Lishan fault.

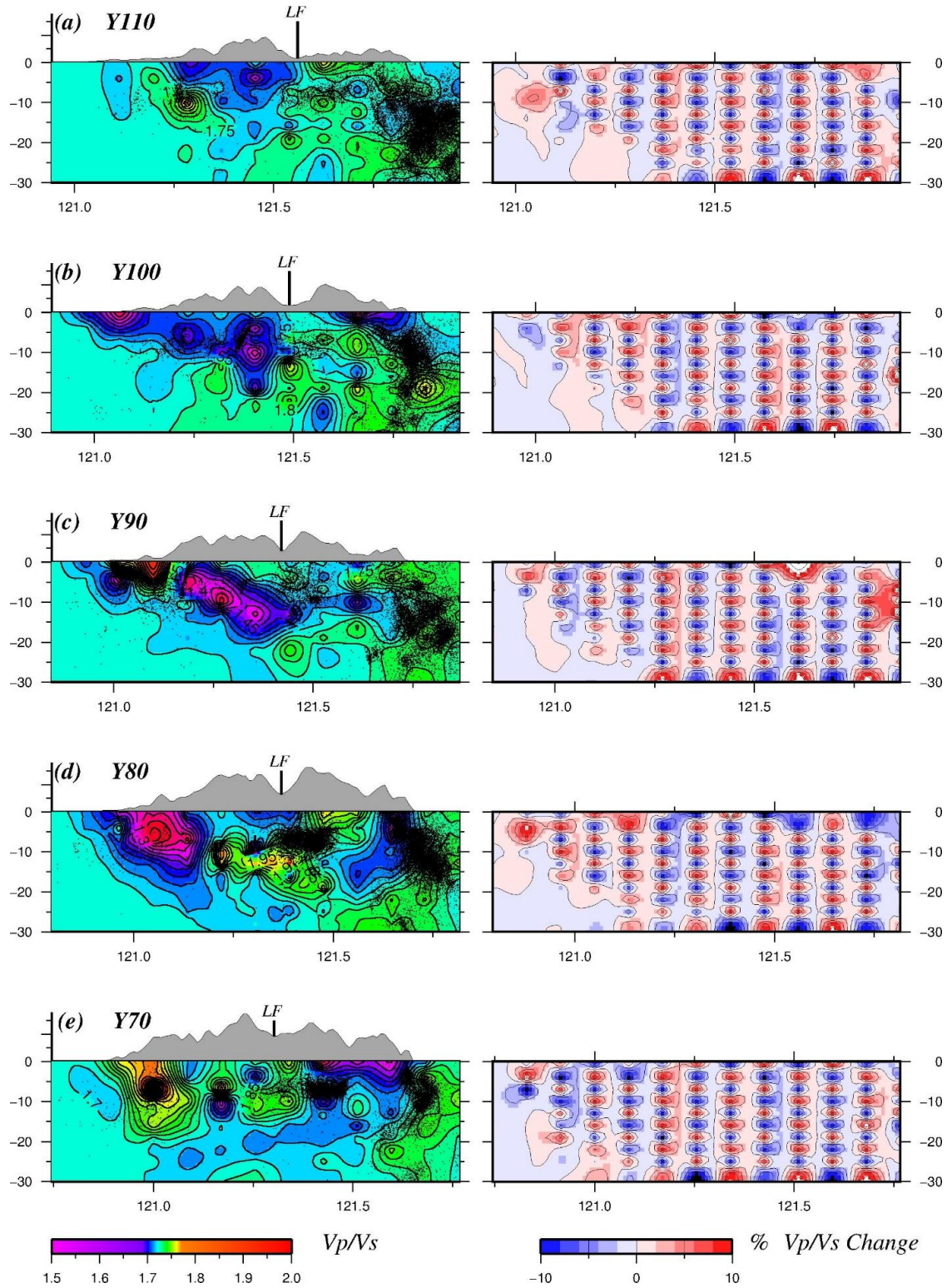


Figure 8. 7 km depth sections through the P-wave model (a), V_p/V_s (b), and (c) magnetic anomalies. Focal mechanism of 14 events with depth less than 10 km and magnitudes greater than 4.5 are also plotted.

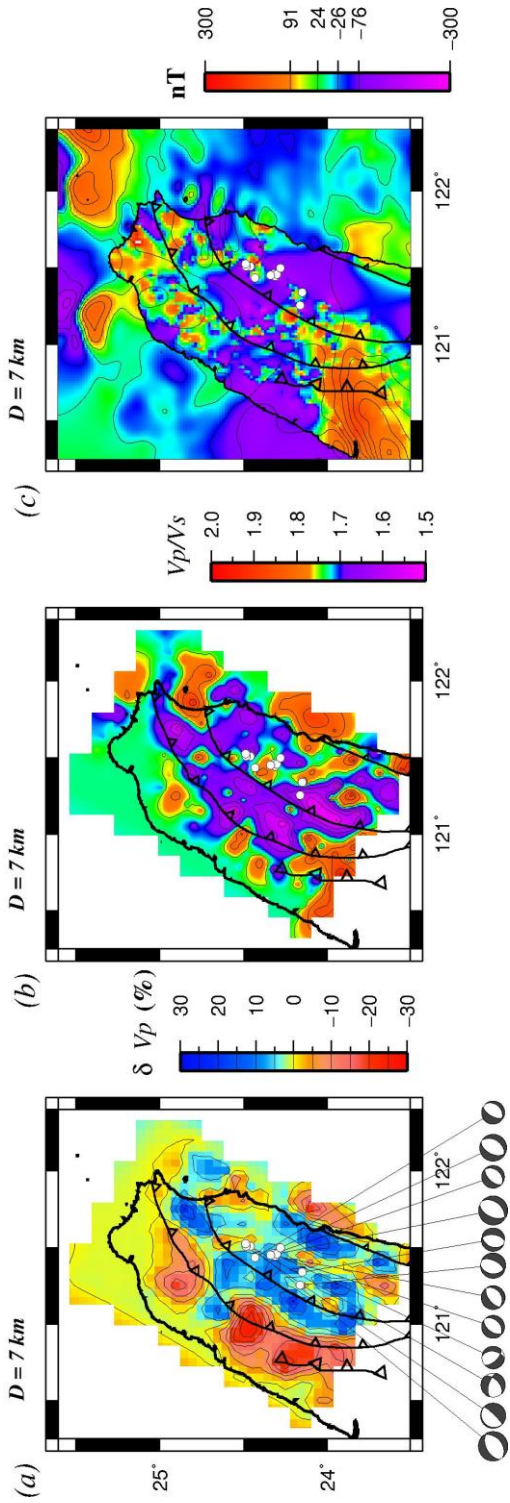


Figure 9. Frequency-magnitude plot for events occurred from 1991 to 2015 in the specify polygonal regionaround the Lishan Fault region. The least-squared formula and the estimated b-value 0.98 are shown at the top.

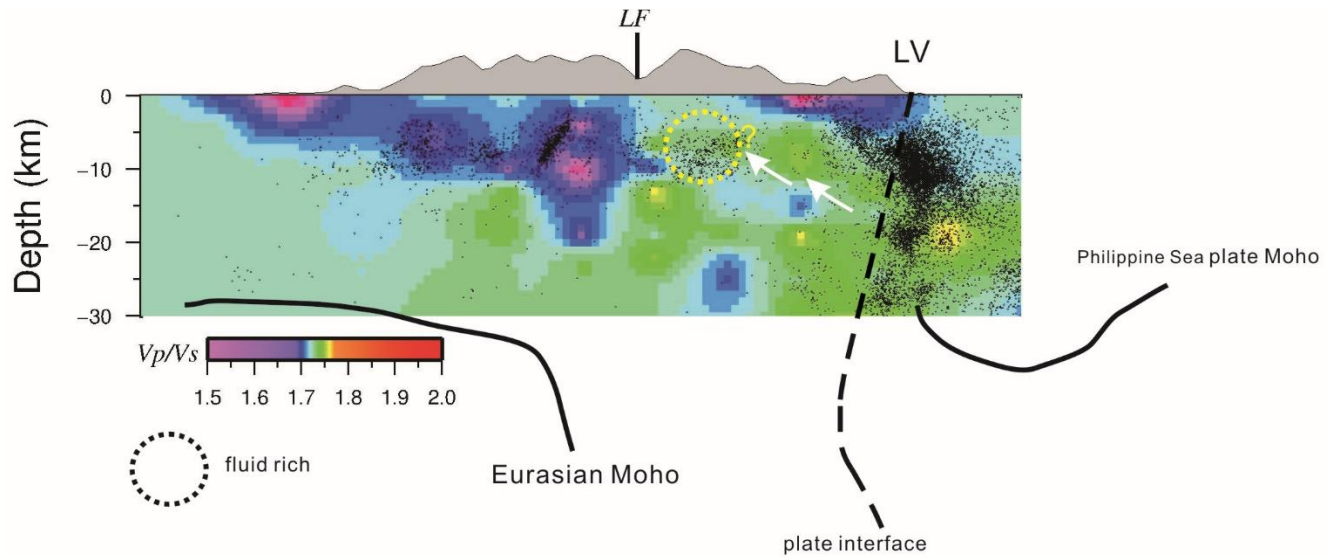


Figure 10. Schematic diagram of a model based on the interpretation of the tomographic profile along Y100 (Fig. 7c), showing possible fluid pathways to the Lishan fault cluster. Thick solid lines marks the interpreted Moho derived by Ustaszewski et al. (2012). LF – Lishan fault; LV- Longitudinal Valley.